7) A. PREUMONT, A. PAY and A. DECAUWERS
The Seismic Analysis of a Free Standing FBR Core.
(A Case Study - SNR-2 Preliminary Design).
Nuclear Engineering and Design, 103 (1987), 199-210.

8) A. PREUMONT, A. PAY and A. DECAUWERS.
Seismic Analysis of a Large FBR Core. Some SNR-2 Preliminary Calculations.
SMIRT-9, Paper E1/7, Lausanne (CH), August 17-21, 1987.

Seismic Analysis Methods for LMFBR Core and Verification with Mock-up Vibration Tests

Y.Sasaki*, T.Kobayashi*, S.Fujimoto*,
M.Morishita**, K.Iwata**, and A.Imazu**

* TOSHIBA Corporation
** Power Reactor and Nuclear Fuel Development Corporation

PAPER NR. 16

1 Introduction

This paper deals with the vibration behaviors of a cluster of core elements with the hexagonal cross section in a barrel under the dynamic excitation due to seismic events.

When a strong earthquake excitation is applied to the core support,the cluster of core elements displace to a geometrical limit determined by restraint rings in the barrel ,and collisions could occur between adjacent elements as a result of their relative motion.

For these reasons, seismic analysis on LMFBR core elements is a complicated non-linear vibration problem,which includes collisions and fluid interactions.

In an actual core design,it is hard to include hundreds of elements in the numerical calculation.

In order to study the seismic behaviors of core elements,experiments with single row 29 elements (17 core fuel assemblies, 4 radial blanket assemblies,and 8 neutron shield assemblies) simulated all elements in MONJU core central row ,and experiments with 7 cluster rows of 37 core fuel assemblies in the core center were performed in a fluid filled tank, using a large-sized shaking table [1].

Moreover,the numerical analyses of these experiments were performed for the validation of simplified and detailed analytical methods.

2 Simplified analytical method

2.1 Study on simulation model

The core elements are assumed to be elastic beams with a hexagonal cross section.The dynamic analyses were performed by use of the direct integration method, in order to precisely express a variation in element vibration mode, due to the collision forces between elements.

In general,increasing degrees of freedom for the numerical model should improve the accuracy of calculations,although the large degree model increases the calculation time.Therefor, modeling requires careful consideration on the individual elements in the simulation model, based on the observation of the natural frequencies.The 1st and 2nd mode natural frequencies are sufficient to predict the response of the core elements satisfactorily judging from the frequency spectrum of excitation wave at the core support structure.

As is obvious from the results of MONJU core element property tests,the 1st mode natural frequency is dependent upon the element amplitude due to the element support clearance effects, as shown in Fig.1. However,it should be pointed out that the a verage displacement amplitude for the investgation may be over 10mm, in connection with the seismic design of core elements.Figure 1 shows that the natural frequency approaches a gradually to a constant value at over 10mm displacement amplitude. So,it was concluded that the linear support model was practically applicable, where the amplitude became large enough, due to the strong excitation.The double simple supports were assumed at the element feet.Moreover,in order to simplify the model, a fixed support condition at the feet could be found. However,it tended to be conservative in regard to the moment response. The fluid effects, due to the presence of sodium among elements and at the sides of the core could be simulated by added masses.Figure 2 and 3 show acceleration response curves for the element top in water by sinusoidal sweep waves.The exiciting frequency range is up to 20Hz according to the considerations on the predominant earthquake vibration frequencies.As is clear from the figures,the response curves have two predominant peaks, that correspond to the 1st mode and the 2nd mode natural frequencies.Moreover,it is noted that one peak occurs in connection with 1st mode of the beam with the fluid interaction.

In Fig.2,the frequency that gives the maximum response corresponding to the 1st mode varies with the input acceleration level.This is a particular phenomena in the beam vibration system with gaps.There is a natural frequency which comes from the relation between gaps and input acceleration level.From these results,it is pointed out that only the effects of diagonal terms in added mass matrix are necessary for the calculation,without increasing calculation time by considering the non-diagonal terms.

All the dissipative effects, which are related with the element structure, fluid and friction, are assumed to be included in damping coefficients.

The assumption of Rayleigh damping is quite effective to simulate the dynamic response by the direct time integration.

Therefore,damping matrix is;

$$[C]=\alpha[M]+\gamma[K] \qquad (1)$$

$$hi=(\alpha+\gamma\omega i^{2})/2\omega i \qquad (2)$$

Where [C] ; Damping matrix

[M] ; Mass matrix

[K] ; Stiffness matrix

hi ; Damping coefficient for i-th mode

ωi ; Natural frequency for i-th mode

α, γ ; Determined from the first two modal damping coefficient

At the possible collision nodes,the collision phenomena between elements are described by equivalent spring-damper systems with initial gaps. Collision forces are calculated by spring deformation.The equivalent spring constant was determined by means of the static load test and the FEM static calculation with the collision pad portion.The equivalent damping coefficient was determined from the restitution coefficient(e);

$$h\fallingdotseq(1/\pi)\ln(1/e) \qquad (3)$$

Restitution coefficient e for the pad portion was measured by striking the pad with a small ball, with restitution coefficient nearly 1.0. During the striking,the pad portion did not go in motion.The restitution coefficient was obtained by the ratio of the speed before and after the ball striking.However,the collision peak force and duration are very sensitive for above equivalent spring-damper system parameters.Therefore,they must be determined carefully.

2.2 Analysis for Mock-up Vibration Tests

In an actual core, hundreds of elements with hexagonal cross section are arranged closely in a barrel. For the experiments, the single row apparatus with 29 elements simulated all elements in the core central row, and seven groups of row apparatus with 37 elements in the core center, were made.

The object for vibration tests and verification analysis are shown in Fig.4 and test apparatuses are shown in Fig.5 and 6.

Figure 5 shows the single row test apparatus, a water tank 4800mm in height and 300*385mm in sectional area. Figure 6 shows the group test apparatus, a water tank 4860mm in height and 1050mm in diameter.

The reasons for making different apparatus configurations were to enable understanding details about the phenomena regarding the single row and the group row, and finally to confirm that the single row analysis represents the design analysis.

A vibrational equation for core elements is expressed as Eq.1.

$$M\ddot{U}+D(\dot{U})+S(U)=-M^{*}\ddot{Z} \qquad (4)$$

Where

M ; Mass matrix, including real mass and added mass

M^{*}; Mass matrix subtracted displaced mass from real mass

D($\dot{U}$) ; Damping matrix as a function of $\dot{U}$

S(U) ; Internal force matrix as a function U

$\ddot{U},\dot{U},U$; Relative acceleration, Velocity, and Displacement

In order to simplify the equation, additional non-linear terms representing the collision forces are added to the right hand side of the equation as external forces. This is the so-called pseudo-force approach.

The modified equation of motion is expressed as Eq.2,

$$[M]\langle\ddot{U}\rangle+[K]\langle U\rangle+[C]\langle\dot{U}\rangle=-[M^{*}]\langle\ddot{Z}\rangle+F \qquad (5)$$

Where $[K]=\partial D/\partial U$, $[C]=\partial S/\partial\dot{U}$

F; Pseudo force

The collision forces become;

$$\begin{Bmatrix} Fi,j \\ Fi+1,j \end{Bmatrix}=\begin{vmatrix} Kc & -Kc \\ -Kc & Kc \end{vmatrix}\begin{Bmatrix} Ui,j \\ Ui+1,j \end{Bmatrix}+\begin{vmatrix} Cc & -Cc \\ -Cc & Cc \end{vmatrix}\begin{Bmatrix} \dot{U}i,j \\ \dot{U}i+1,j \end{Bmatrix} \qquad (6)$$

Where Kc and Cc are equivalent collision spring and damping, respectively. Here, i represents element index and j denotes node

Kc and Cc have non-linear characteristics, with respect to relative displacement $\delta=Ui,j-Ui+1,j$.

A detailed analytical model example considering the variation of cross section along the axis of an element for the single row 29 elements is shown in Fig.7.

A huge amount of computational time and memory capacities are required to solve such a detailed model by use of the direct integration method. Therefore, the simplified model was adopted, as shown in Fig.8.

In this calculation model, mass points were selected at the collision pads.

As for the method for mass reduction model, the static condensation method well known as the Guyan Reduction Method [2], and the flexibility influence coefficients method are considered to be useful.

To analyse the core elements seismic response, it is necessary to obtain the core support structure acceleration time history for the earthquake, which is shown in Fig.9. Furthermore, the displacement response spectrum is shown in the figure.

Figure 10 shows the displacement response time history for the elements. This result was obtained under 400gal excitation in water. In the figure, element No.1 is located at the side of the single row and element No.15 is located at the center of the row. Each element has a geometrical displacement limit at the element top pad and the middle pad.

The relationship between maximum displacement distribution at element top and geometrical limit is shown in Fig.11. As is obvious from the figure, the elements reach a half of the geometrical limit under 400gal excitation. Therefore, about two times the excitation level is required to reach the geometrical limit.

The analytical results agree with the experimental results within practical applications.

Figure 12 shows the experimental and analytical results for the maximum response stress of elements. In regard to the stress at the support, a discrepancy appeared between the analytical results and the experimental results. It was assumed that the discrepancy is attributed to the linear support model at the element feet, as mentioned previously in 2.2. However, it is difficult to estimate the clearance at the feet under construction.

The discrepancy may reduce with the displacement increase.

The 37 fuel assemblies in the group test were arranged in a symmetric cluster and contained in a circular tank. Restraint rings were provided in the tank to limit the average gap between elements to 0.7mm at the top and 1.0mm at the middle part.The purpose of this test was to study the effects of a three dimensional array for comparison with the single row model test. The group 37 elements model is considered to be as much like a reduced scale model of an actual core diameter direction.It is impossible to analyse the entire core with a large degree of freedom, including collisions and fluid interaction.Therefore,another idea is required.It is applicable to attempt the examination of the prospect represented by the single row model for the whole core model.Interest in the group model is focussed on the fluid force estimation.As the size of gap between elements and at the sides of core decrease,the fluid added mass increases further and decreases the element response by reducing the fluid participation factor against earthquake excitation.For the numerical evaluation of the added mass matrix,the Laplace equation was solved by means of FEM |3|.For an additional fluid damping evaluation,the viscosity of fluid was taken into account and the linearized Navier-Stokes equation was solved by means of FEM |4|.However, numerical efforts were confined to small scale array models.The simplified evaluation model, which is shown as a macroscopic model in Fig.13,is required for the hundreds of elements in an actual core.

In Fig.13,r_e is the inside diameter of the rigid tank, and r_i is the radius of an equivalent cross-sectional area of the core, which is equalized to an outline area of the elements.

Space ratio (ε) in the elements is defined as,

$$\varepsilon=(N-1)\delta/\{(N-1)\delta+N*\sqrt{3}a\} \qquad (7)$$

Where N is number of gaps in the central row, δ is gap width and a is the length of the side of hexagonal duct.

The added mass for the principal vibration mode is,

$$Mv=\{(1-\varepsilon)(r_e^2+r_i^2)\}/\{(1+\varepsilon)r_e^2-(1-\varepsilon)r_i^2\}*Md \qquad (8)$$

$$Md=\rho Nt*3\sqrt{3}a^2/2$$

Where Md is the displaced fluid mass, ρ is density of fluid and Nt is the number of core elements. As an application of the above method,the group 37 elements model in Fig.13 was considered.

Structural parameters in Fig.13 are shown as follows;

$\delta/a=0.078$, $r_i/r_e=0.56$

N=6 , Nt=37

Then,the added mass was obtained ;

$Mv=1.7Md$, $Md=96.1a^2\rho/g$

By use of above results,the natural frequency of group elements in water was estimated.The calculated result, 2.5Hz was in satisfactory agreement with experimental result of 2.4Hz.

In accordance with the investgation already mentioned,the non-diagonal terms of added mass matrix are not taken into account in the present analysis.As is obvious from Eq.1,the seismic excitation is decreased by an amount equal to like the buoyancy force, which relates the external force of the right hand side of equation.This effect should be taken into account.

The core designer must give thought to the entire core analysis procedure, with accuracy for practical usage and with computational time economy.Therefore,the single row 7 elements model analysis was substituted for the group 37 elements analysis.The exciting acceleration time history is the same as for the single row 29 elements analysis.The acceleration level is 600gal to set the level for the experiment.

The time history of displacement response is shown in Fig.14, comparing experimental results with analytical results.Gaps between the elements are 0.7mm at the top pad and 1.0mm at the middle pad.So,the geometrical limits by the restraint rings are 4.9mm at the top and 7mm at the middle pad.The elements displace to the geometrical limit.

Figure 15 shows the time history for strain in experiment. Figure 16 shows the bending moment in analysis.Different behaviors come out at each location of the element in the stress response.They are due to the displacement restriction at the top pads by the restraint rings.The time history shows that a 1st mode is generally predominant at the element support,a 12Hz component included in the input wave is predominant at the middle part,and a high frequency component due to the collision is predominant at near the top respectively.

The analysis closely simulates the behaviors in the experiment.

The maximum stress distribution is described in Fig.17.Element No.1 is located at the side and element No.4 is located at the center.

It is noticed that the stress in the middle part increases relatively, compared with the stress in single row cases.The cause for the increasing stress may be the restriction on top displacement, due to the displacing to the geometrical limit.That is, the vibration mode for the giving maximum stress may change severely for the middle part.

The discrepancy between the analytical results and the experimental results in regard to the upper part stress comes from the estimation accuracy of the collision peak forces. In the design calculation,an effective mass correction factor can be useful in solving the problems.

Figure 18 shows the change in 1st mode natural frequency in air excitation. The horizontal axis of the figure means the acceleration divided by the total gap value in the row.The change in frequency due to the input acceleration is the same in the single row model and the group model.

3 Conclusions

The results of studies lead to the following conclusions;

(1) The simplified analytical model could simulate the element behavior in a certain degree of approximation,and a conservative response could be obtained as a result.

(2) The single central row model could give a practical representation for a design calculation for the whole core elements,with consideration of fluid forces and dampings.

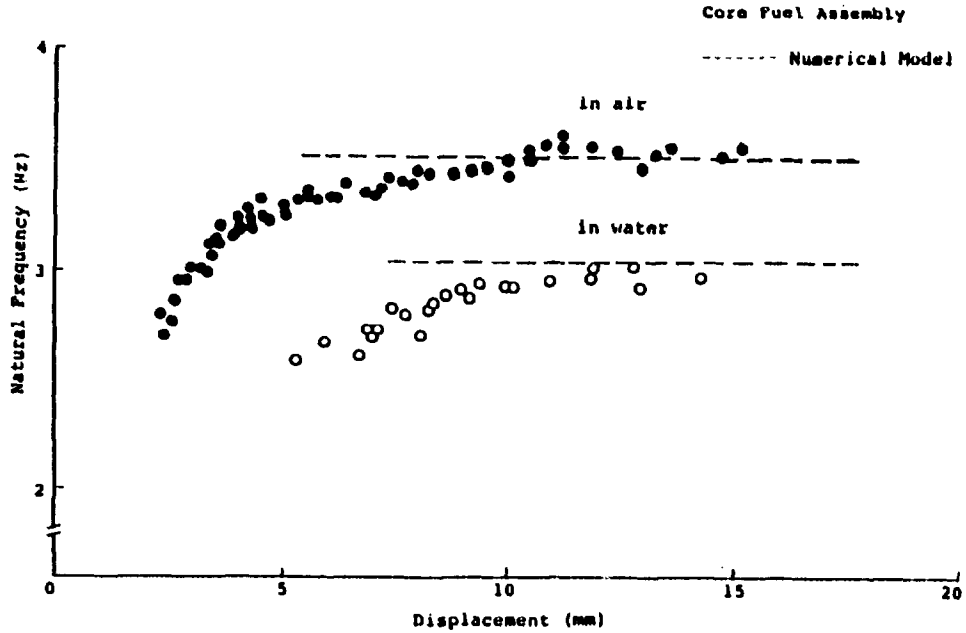

Fig.1 Maximum Response Frequency Measured in Air and Water Vs.Displacement

References

[1] Sasaki,Y.,and Muto,T.,"Experimetal Studies on Seismic Vibration Phenomena of FBR Core Components" 7th SMiRT,F7/3

[2] Guyan,R.J.,"Reduction of Stiffness and Mass Mmatrix" AIAAJ.,Vol.3,1985,380

[3] Preumont,A.et al.,"Fluid-Coupling Coefficient in an Array of Hexagonal Prisms" Nuclear Engineering and Design 92,1986

[4] Yang,C.I.,and Moran,T.J.,"Calculation of Added Mass and Damping Coefficients for Hexagonal Cylinders in a Confined Viscous Fluid" Transaction of ASME 152,Vol.102,May,1980

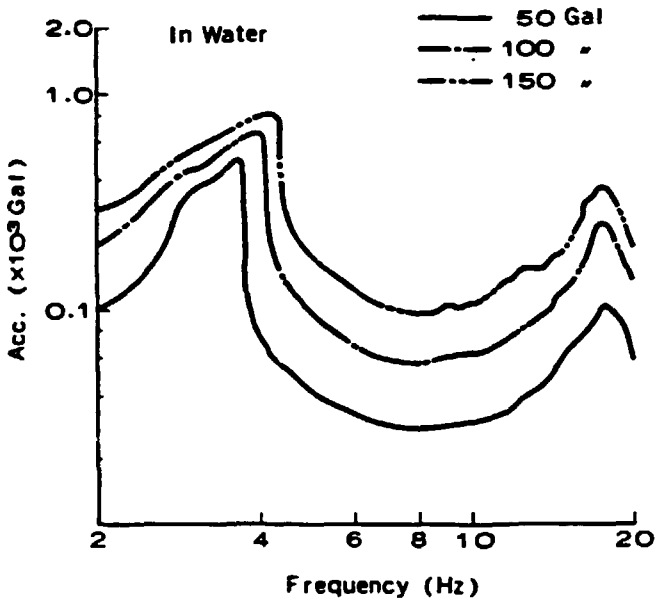

Fig.2 Response Curves for Element in Single Row Model

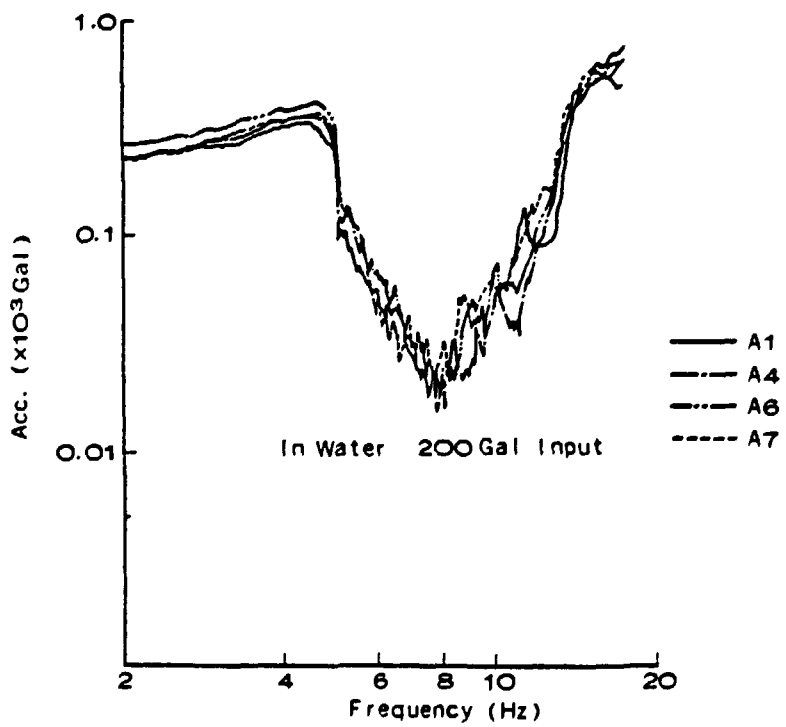

Fig.3 Response Curves for Element in Group Model

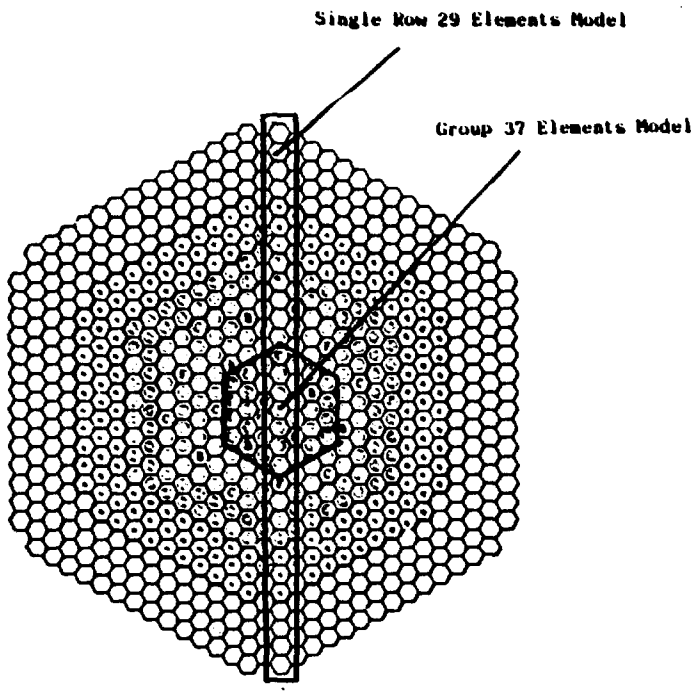

Fig.4 Configuration for Mock-up Vibration Test and Verification Analysis

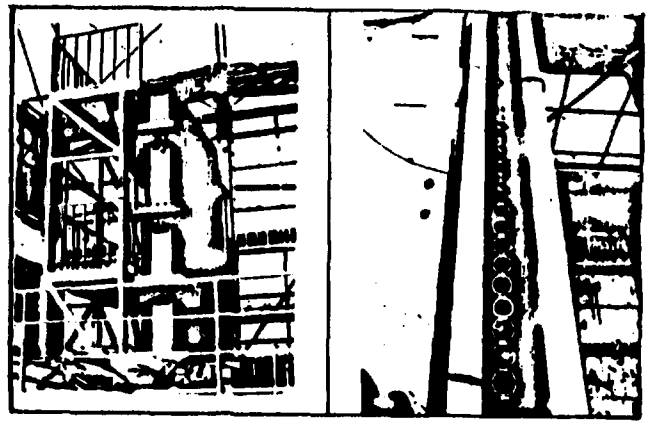

Fig.5 Single Row Test Apparatus

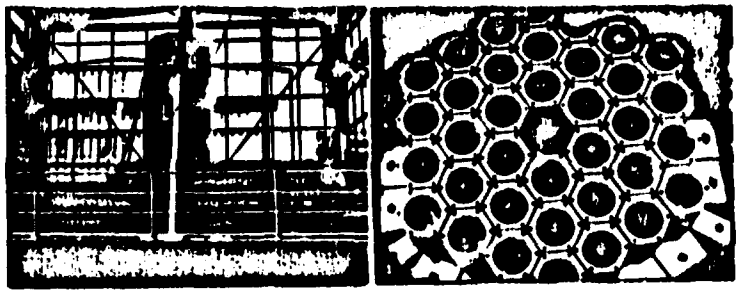

Fig.6 Group Test Apparatus

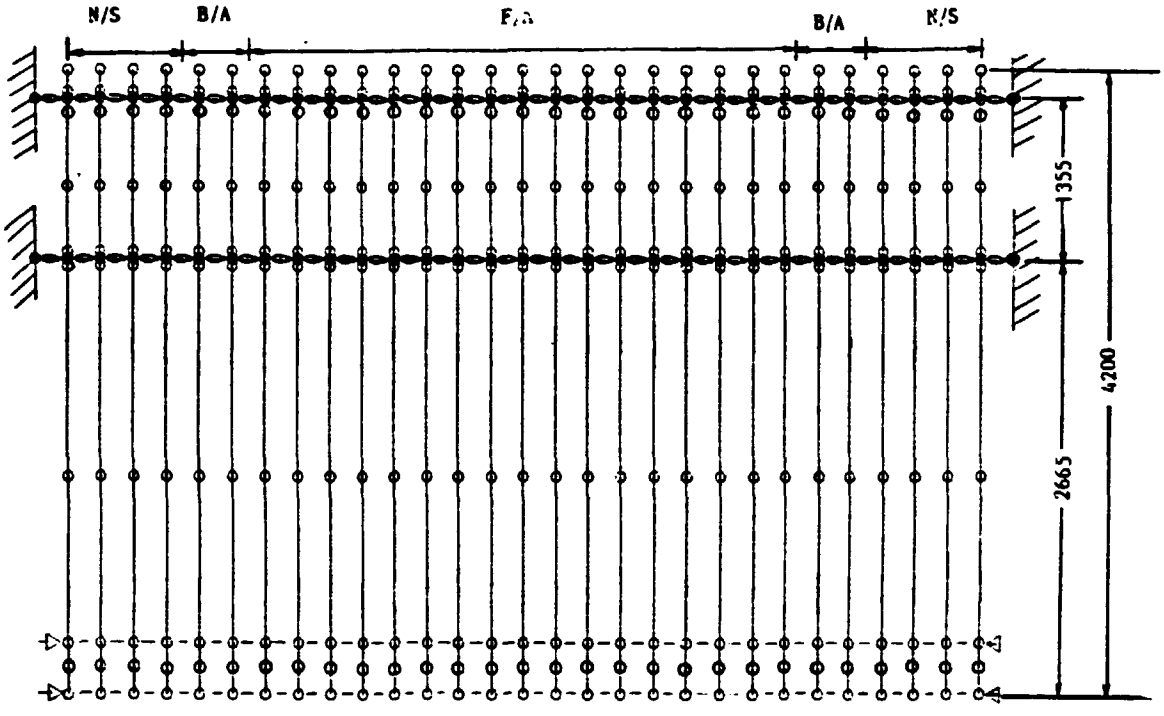

Fig.7 Detail Analytical Model

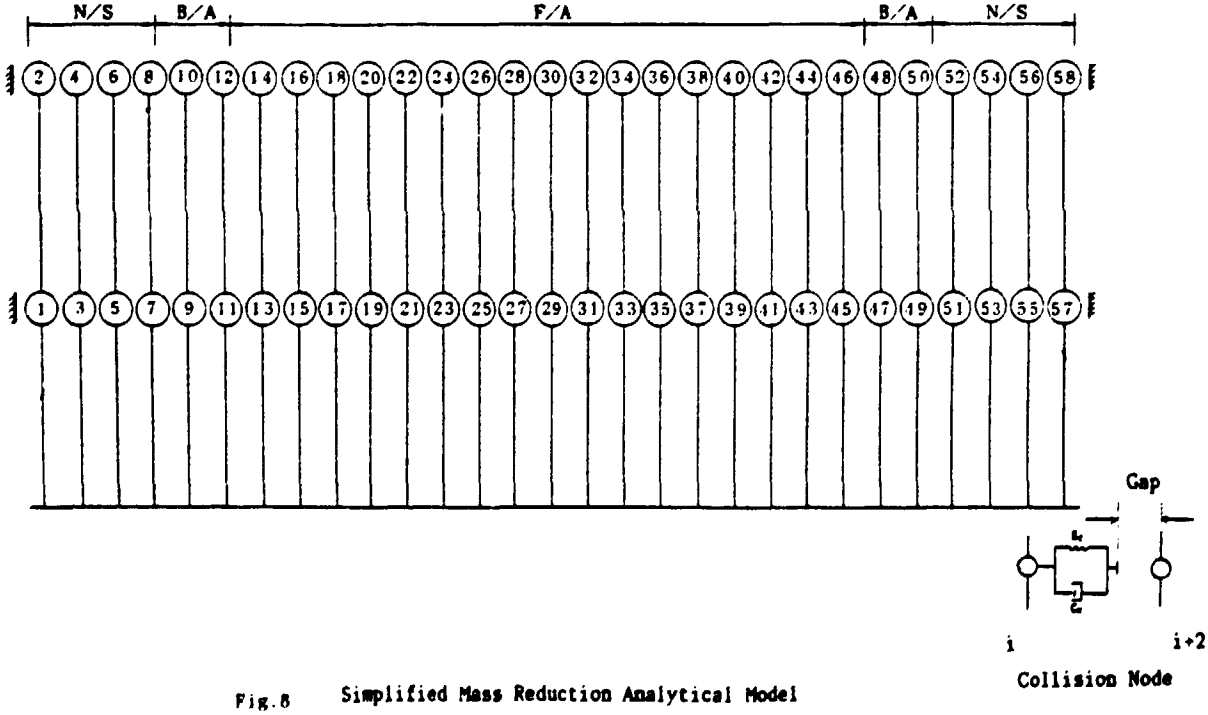

Fig.8 Simplified Mass Reduction Analytical Model

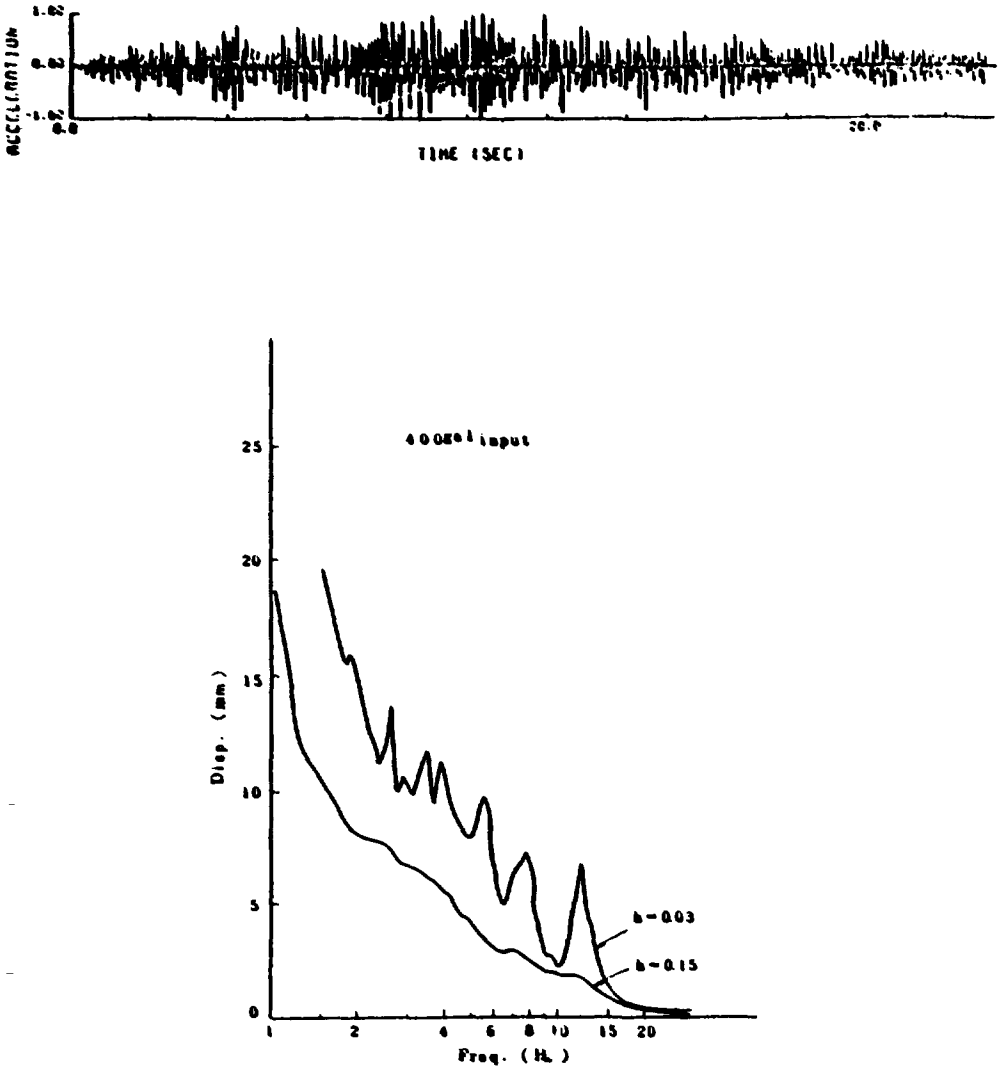

Fig.9 Time History and Displacement Response Spectrum for Core Support Response Wave under Earthquake Excitation (Input Acceleration Wave)

Unit mm

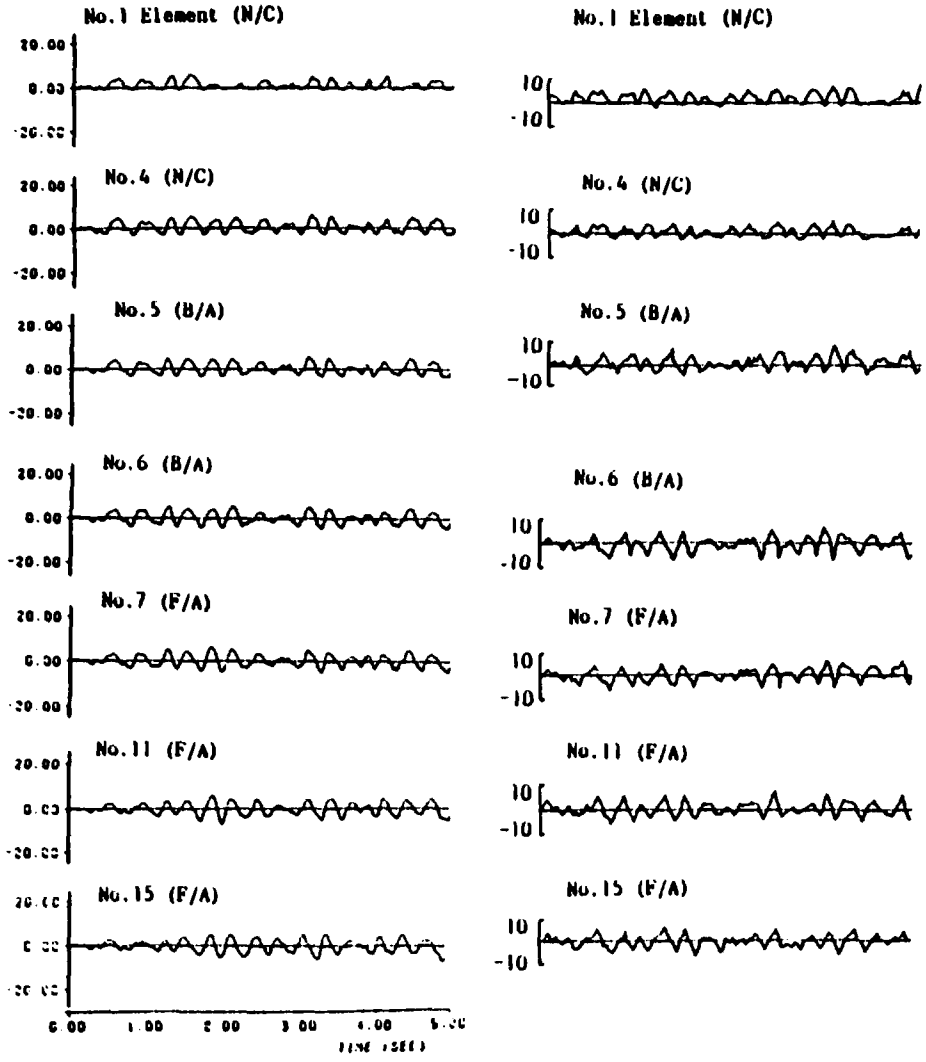

Fig.10 Displacement Time History for Element Top in Single Row 29 elements Model

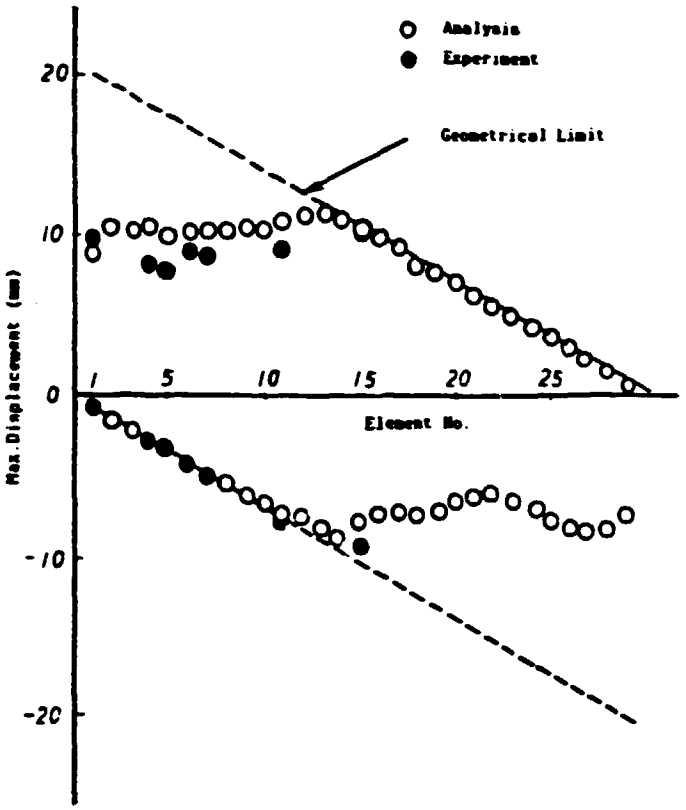

Fig.11 Maximum Displacement Distribution for Element Top in Single Row 29 Elements Test (In Water, 400Gal Excitation)

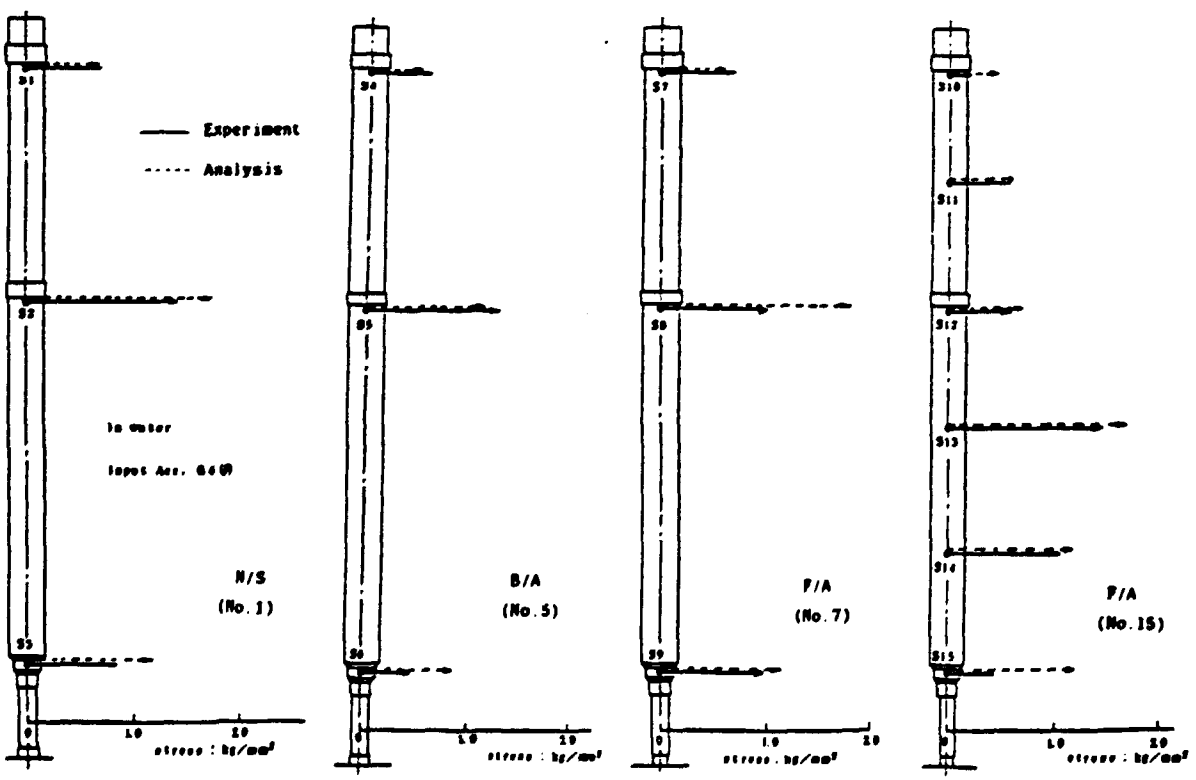

Fig.12 Maximum Response Stress for Elements

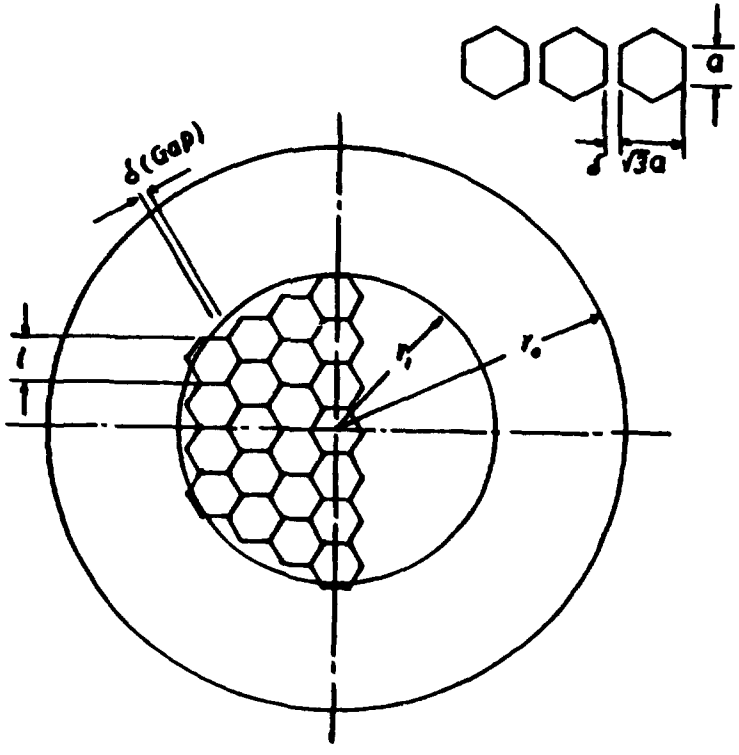

Fig. 13 Macroscopic Model for Calculation of Added Mass Coefficient

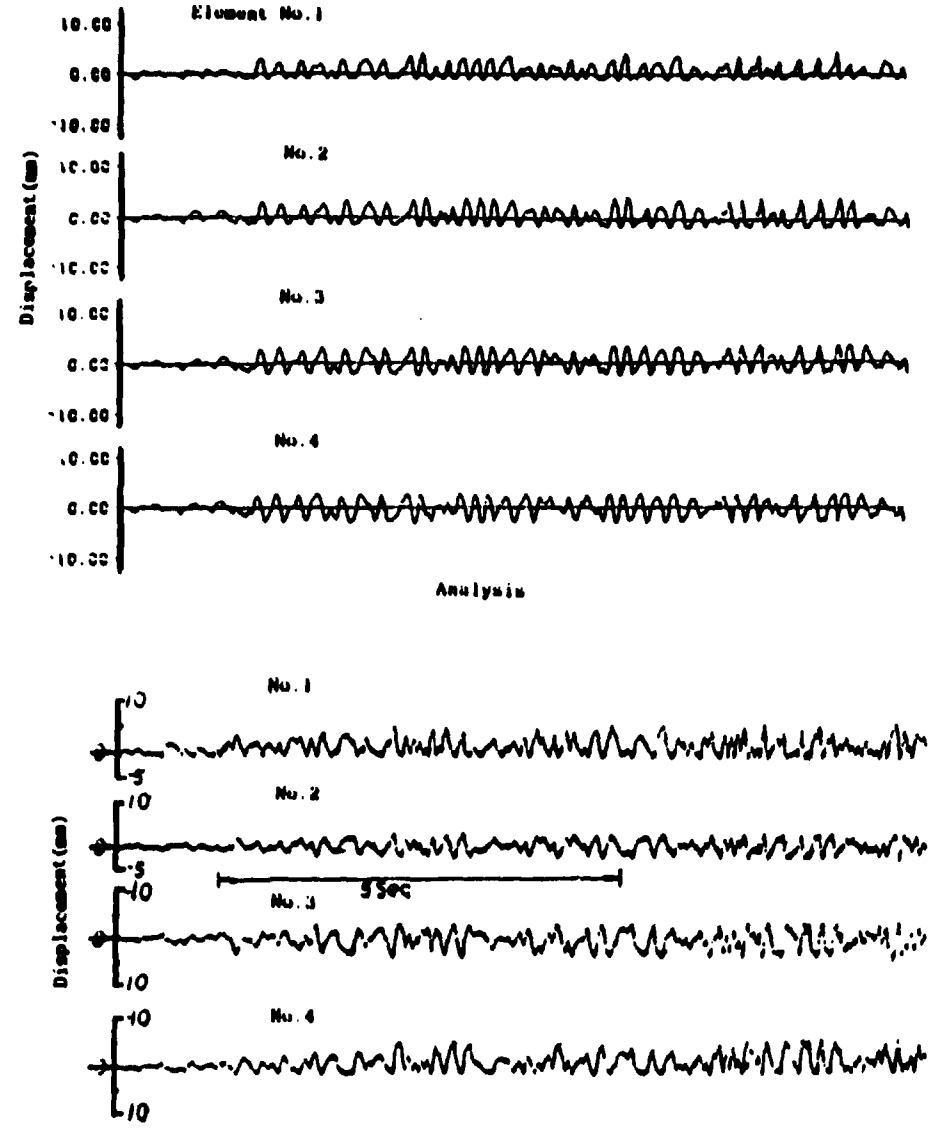

Fig. 14 Time History of Displacement for 37 Elements Model

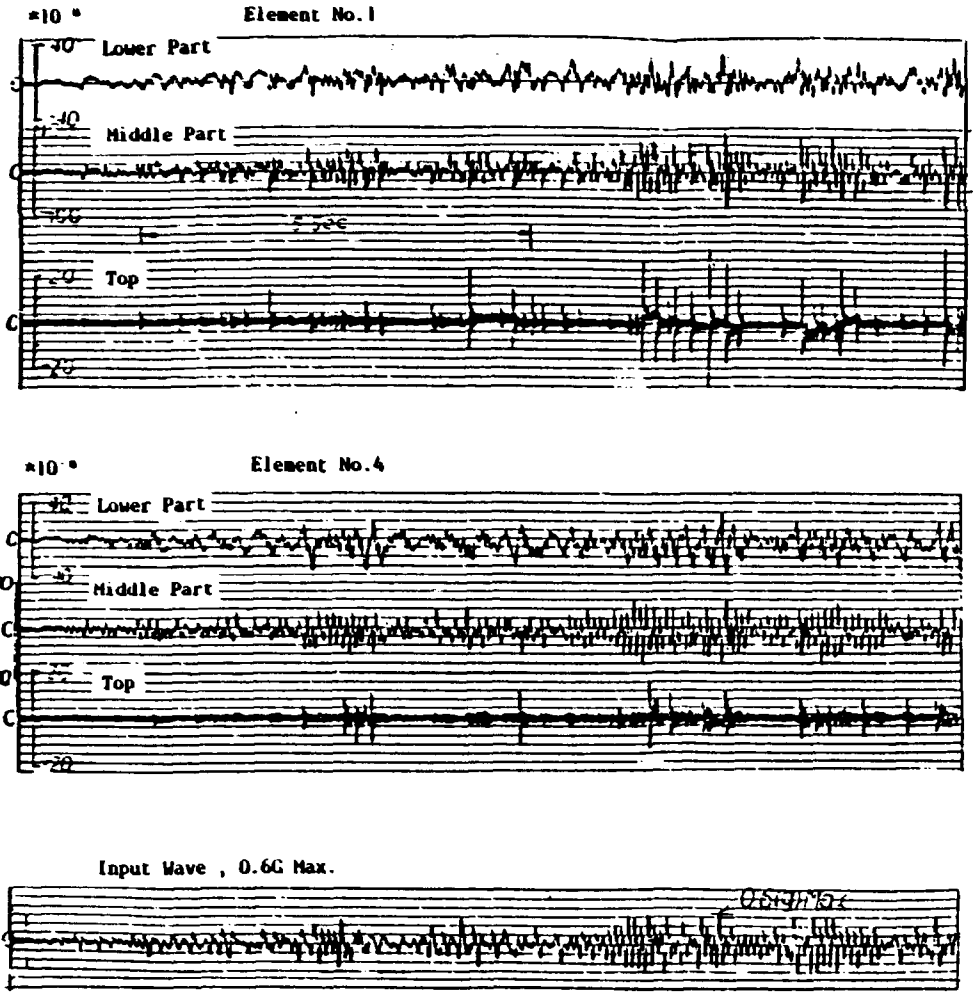

Fig.15 Time History of Strain for 37 Elements Model (Experiment)

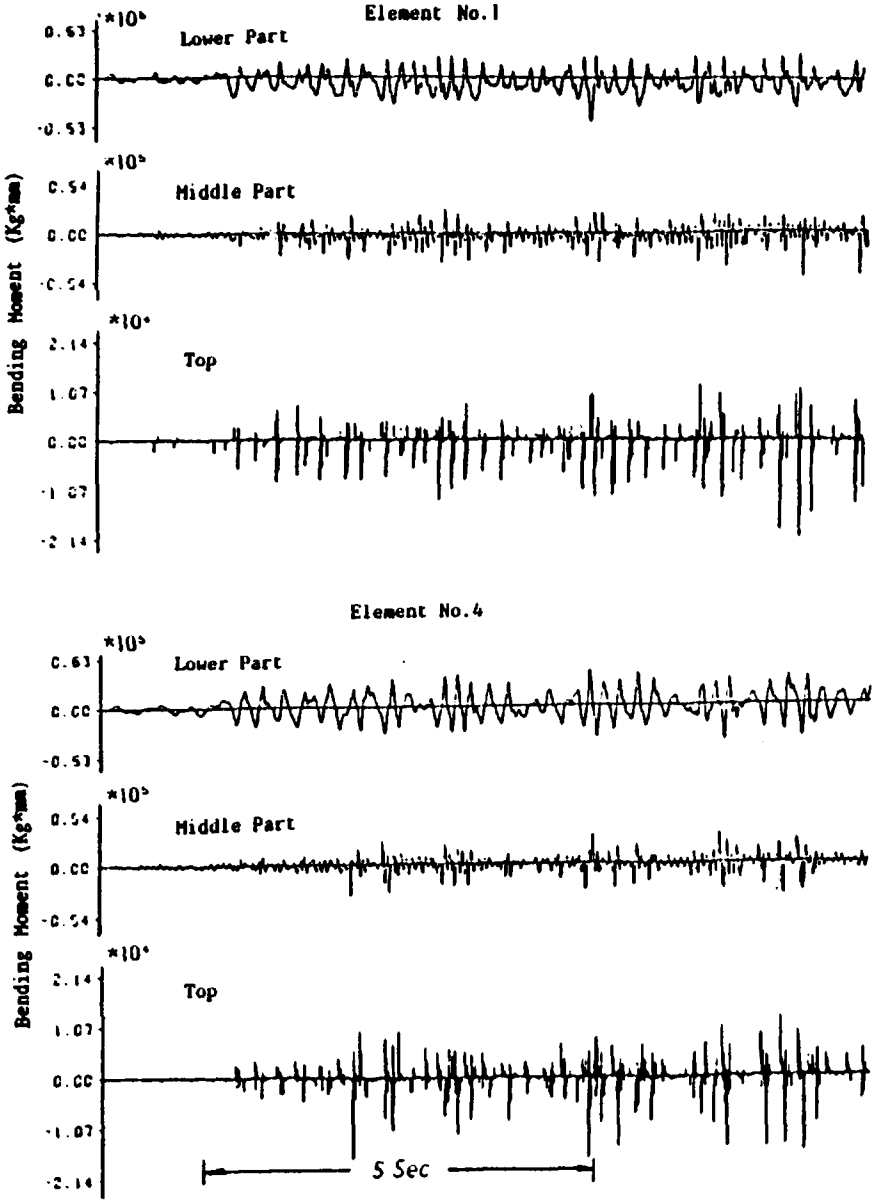

Fig.16 Time History of Bending Moment for 37 Elements Model (Analysis)

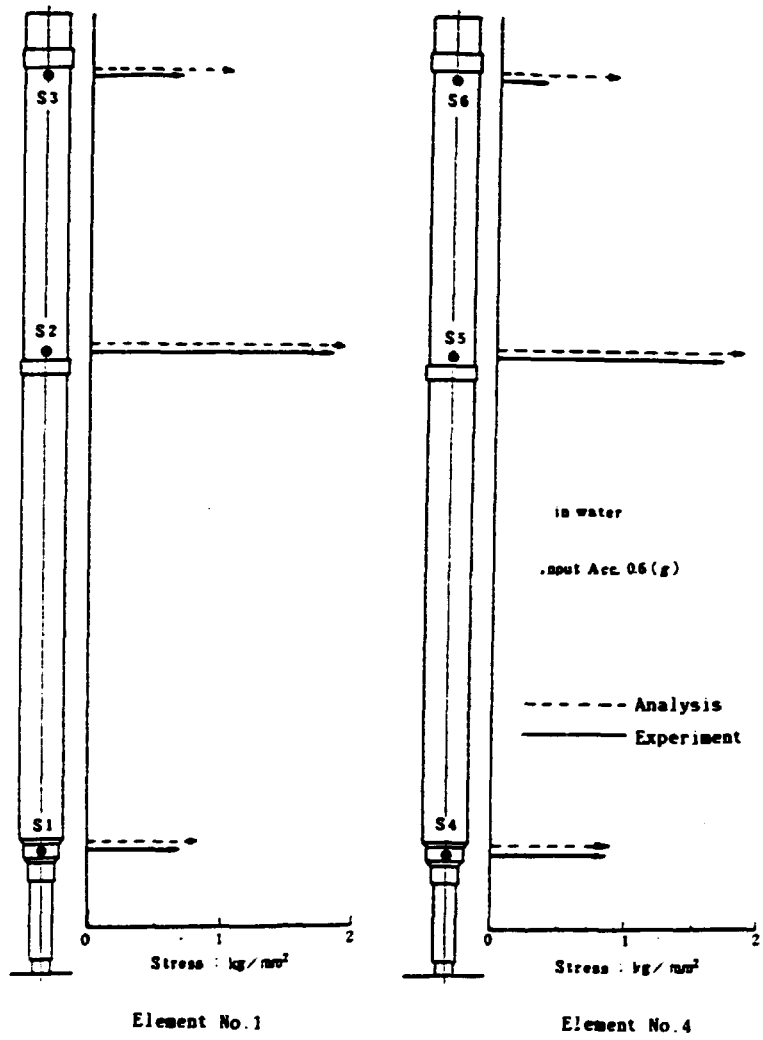

Fig.17 Maximum Stress of 37 Elements Model

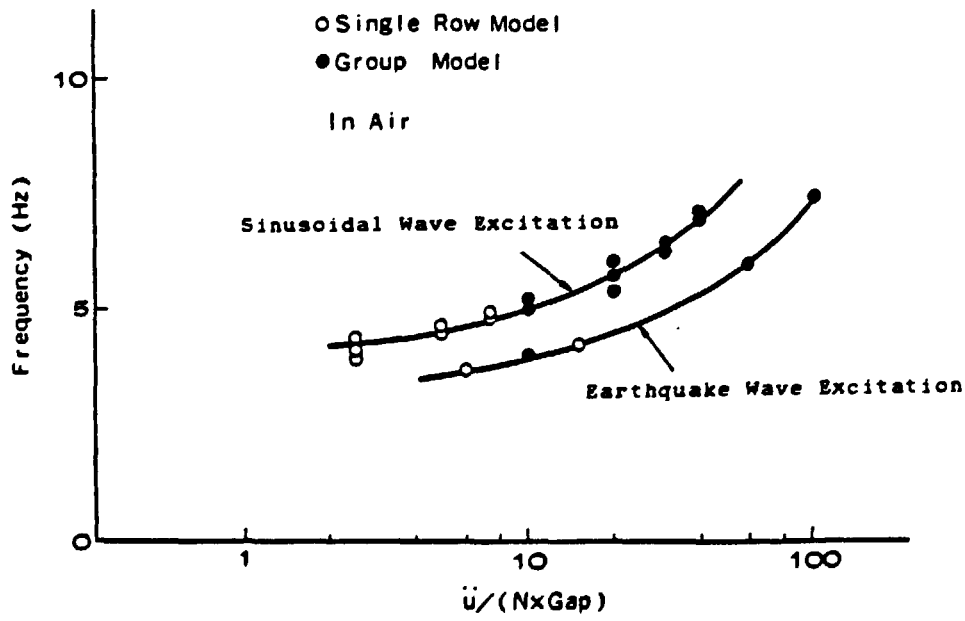

Fig.18 Relation between Input Acceleration and Predominant Frequency